

Supporting Information

Table S1 Cell parameters of parent HZSM-5 and phosphorus-modified HZSM-5 zeolite determined by Le Bail method¹ and quantitative phase analysis by Rietveld method³

Sample	Space group	a (Å)	b (Å)	c (Å)	V (Å ³)	R _v [#]	Crystallinity %
Parent	<i>Pnma</i>	20.1222(4)	19.9280(3)	13.4064(3)	5375.9(1)	100	100
0.8 P/Al <i>b.c.</i> *	<i>Pnma</i>	20.1021(4)	19.9461(4)	13.4214(3)	5381.4(2)		100
0.8 P/Al	<i>Pnma</i>	20.0722(4)	19.9114(4)	13.4048(3)	5357.5(2)	99.6	65.5(7)
5.0 P/Al § <i>b.c.</i> *	<i>Pnma</i>	20.0884(5)	19.9356(5)	13.4431(4)	5383.6(2)		100
5.0 P/Al §	<i>Pnma</i>	20.086(1)	19.8748(7)	13.3610(7)	5333.7(4)	99.2	39.3(7)
Silicon orthophosphate	<i>R-3H</i>	7.857(2)	7.857(2)	24.16(3)	1291.6(9)		2.5(7)

[#] Relative unit-cell volumes

*The designation *b.c.* indicates before calcination

§ Not exposed to ambient humidity

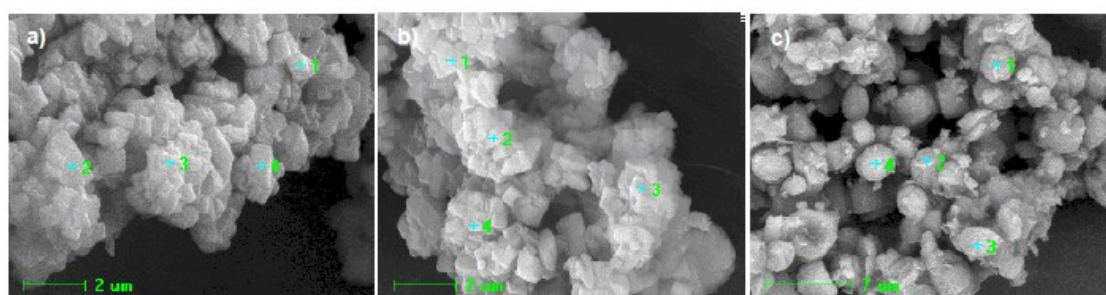


Fig. S1 SEM images of the parent, 0.8 P/Al and 5.0 P/Al samples. The crosses indicate the measuring points taken for EDX analysis.

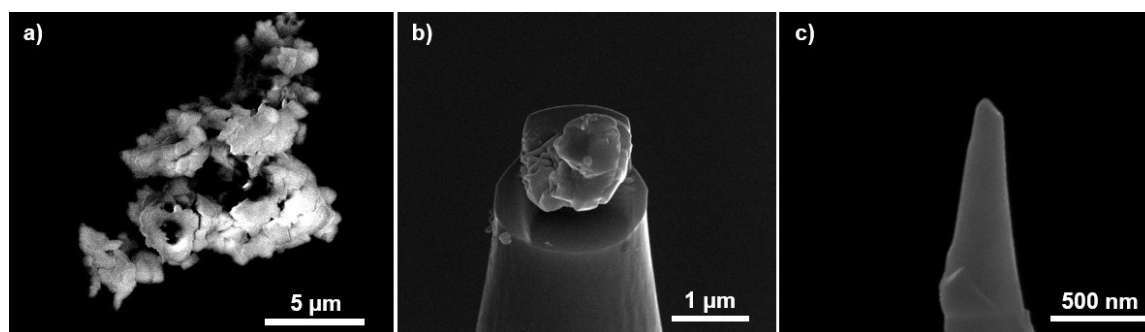


Fig. S2 Scanning electron microscopy images of catalysts and needles for the APT experiment. a) Crystals of 1 P/Al HZSM-5 b) SEM image of P-MFI loaded onto a silicon micropost prior to focused ion beam (FIB) milling. c) SEM image of the needle of P-MFI created by FIB milling prior to the atom probe experiment.

Scanning electron microscopy and focused ion beam milling

Scanning electron microscopy (SEM) for figure S2 has been performed on a FEI Nova 200 Dual-Beam SEM/FIB located within the Center for Nanophase Materials Sciences (CNMS) at Oak Ridge National Laboratory (ORNL). SEM for figure S1 was performed as described in the main text. The microscope is equipped with the following options: FEG scanning electron microscope, Ion column with Ga liquid ion source for milling, GIS for Pt deposition, Kleindiek nanomanipulator for specimen lift-out and AutoTEM, AutoFIB, and slice and view automation software.

Atom Probe Tomography

Needles for APT analysis were prepared using FIB milling, and representative SEM images are shown in Figure S2. Two samples that yielded APT data sets are summarized in Table S1. The zeolite crystal aggregates were too small for standard preparation, so crystals were attached to the liftout needle by electrostatic force and transferred to Si micro tips via ebeam Pt deposition where they were FIB milled into needle-shaped specimens, as shown in Figure S2. The needle specimens were transferred to the LEAP 4000XR local electrode atom probe equipped with laser pulsing capabilities and an energy compensating reflectron lens located within the Center for Nanophase Materials Sciences (CNMS) at Oak Ridge National Laboratory (ORNL). The specimens were run in laser pulse mode with a laser energy of 200 pJ, base temperature of 40 K, pulse repetition rate of 200 kHz, and a detection rate of 1 atom per 200 pulses. The detector has an efficiency of ~37%.

Table S2. Compositions for the needles as determined using atom probe tomography.

Element	Needle 1 atomic %	Needle 2 atomic %
Al	2.5	1.5
O	60.2	65.7
Si	35.0	31.2
P	2.1	1.2
Si/Al	14.0	21.1
P/Al	0.9	0.8

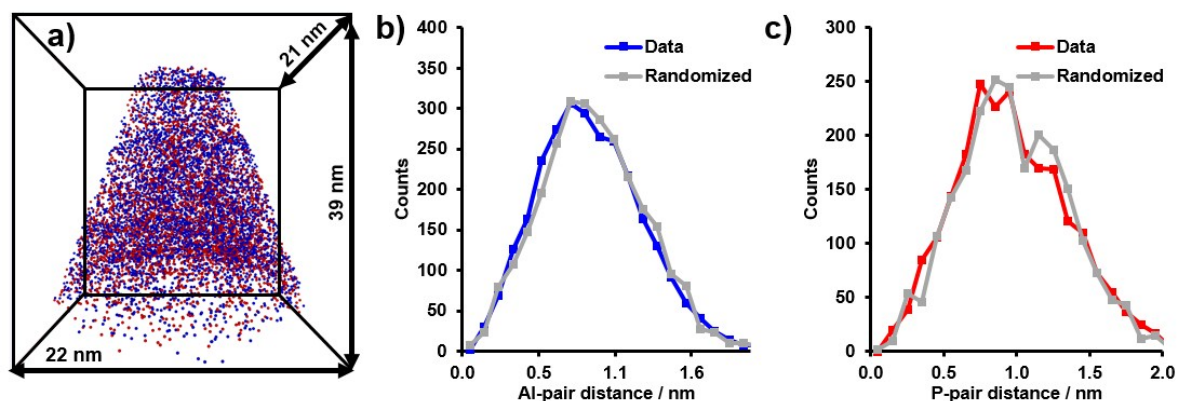


Figure S3. a) Reconstruction of Needle 2 with Al and P atoms shown, and colors as indicated in parts b and c. b) Al nearest neighbor distribution (NND) of the collected data and a randomized data set. c) P NND of the collected data and a randomized data set.

Frequency distribution analysis

Deviations from a random distribution can be statistically evaluated using a frequency distribution analysis (FDA), which was applied using CAMECA's IVAS software. The FDA is discussed in detail in references⁵⁻⁷ and it is used to examine variations in local composition. It is conducted by binning the ions into blocks (block size of 100 was used in this work). Then, a block composition histogram is plotted with the number of bins as the y-axis and concentration as the x-axis. This distribution is then compared to a random distribution of the data determined by a binomial distribution, and a p-test is used to check for statistically relevant clustering (significance level of 0.010 was used). The reduced X^2 test is used to quantitatively confirm or refute deviation from a random distribution, and the Pearson coefficient can determine the severity of the deviation³. The reduced X^2 value is X^2 divided by degrees of freedom. A small value indicates no deviation from a random solid solution. The Pearson coefficient (μ) is defined in reference⁹ and is used to normalize X^2 with respect to sample size and therefore can serve as a more appropriate method to identify clustering because the p-test is increasingly sensitive to small deviations

for large sample sizes, as is the case for APT data. The Pearson coefficient has a value between 0 and 1, where 1 represents a complete association of the identified ions and 0 represents no correlation of the ions.

Table S3. Needle 1 statistical tests to statistically determine the homogeneity or heterogeneity of the elemental distribution. For all elements, the distribution was found to be random.

Element	Reduced X^2	p-value	Pearson coefficient (μ)
Al	0.350	0.8445	0.1230
P	0.394	0.8133	0.1304

Table S4. Needle 2 statistical tests to statistically determine the homogeneity or heterogeneity of the elemental distribution. For all elements, the distribution was found to be random.

Element	Reduced X^2	p-value	Pearson coefficient (μ)
Al	0.696	0.6266	0.0562
P	0.509	0.7292	0.0430

Catalytic testing

The parent and the 0.8 P/Al materials were steamed at 788°C for 5 hours under an atmosphere of 100% steam. The samples were heated in packed bed reactor. The treatment was carried at atmospheric conditions and started at room temperature under a flow of nitrogen (600 ml/min). The temperature was increased at a rate of 40°C/min to 770°C. The ramp rate was then lowered to 5°C to avoid overshoot. At 778°C, the flow of nitrogen was lowered to 200 ml/min. When the setpoint temperature of 788°C was reached, 100% steam was added. The sample was held there for 5 minutes, after which the nitrogen flow was switched off. The sample was steamed at 788°C for five hours. After steaming, the nitrogen flow was restored (200 ml/min), and the sample was held for 5 minutes. After this, steam was switched off, nitrogen flow was increased to 600 ml/min, and the oven was opened to allow more rapid cooling to RT. Approximately 30 mg of each sample was then transferred into a small packed reactor, and subjected to a number of pulses of 0.1 µl of dodecane in helium flow at 600°C. The conversion of dodecane was recorded by gas chromatography (GC) analysis. Samples were measured in duplicate, the parent in triplicate.

Dodecane cracking

As shown in Fig. S4, the blank reactor without catalyst converted approximately 10% of the dodecane pulses. The parent material showed a conversion (corrected for the blank conversion) of 26.5%, the 0.8 P/Al HZSM-5 sample showed a conversion of 69.4%. The first-order rate constants were 2.76 s⁻¹ for the parent and 10.5 s⁻¹ for the P-treated sample. Standard deviations in the conversions were approximately 2%. Selectivities to cracked products were similar for all samples. Activities slightly declined over a series of multiple pulses, but the variation between first and last pulses was not greater than 2%. The catalytic tests clearly show the higher activity retention of the P-treated sample in hydrocarbon conversion after severe steaming.

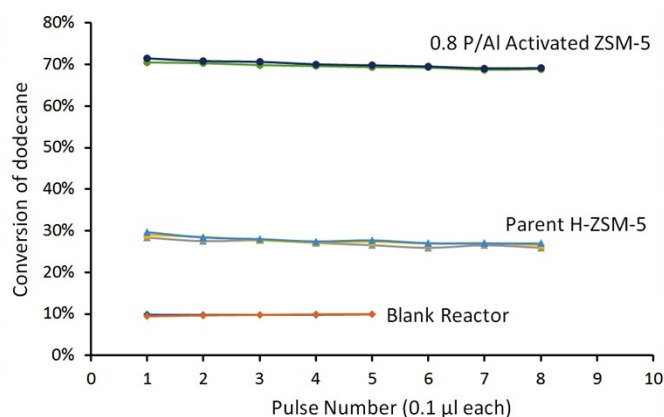
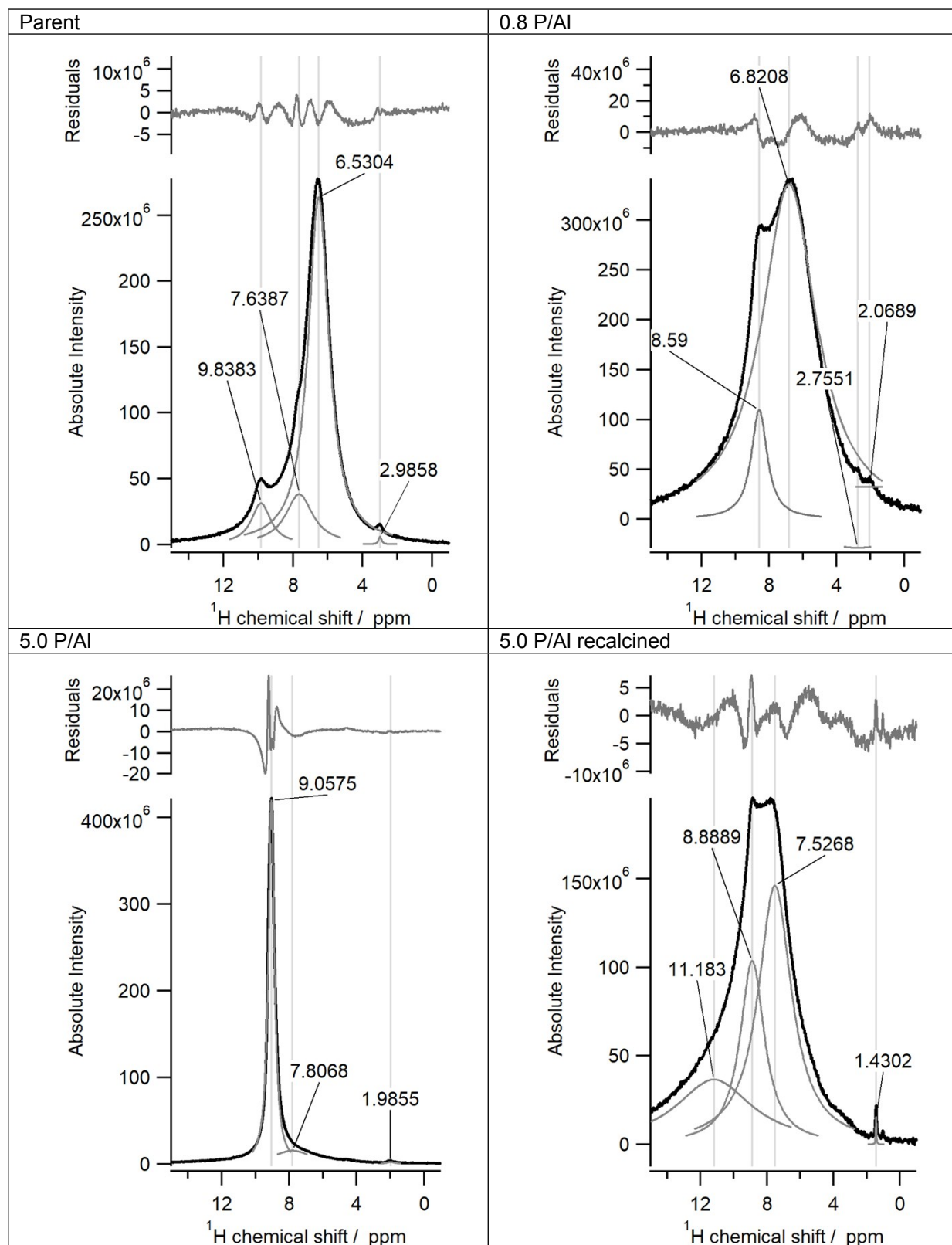


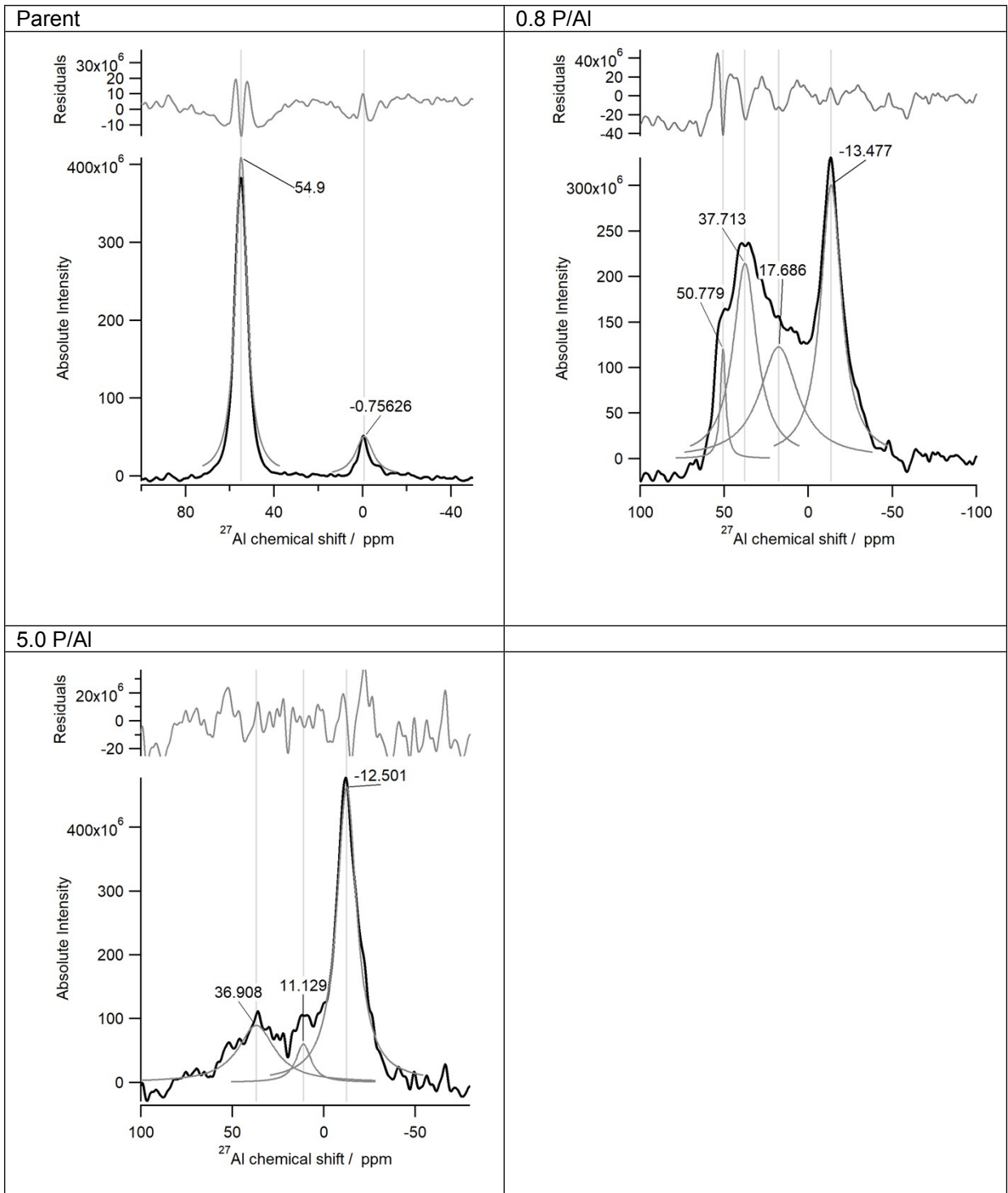
Fig. S4 Overview of the conversion rates of dodecane for blank reactor, parent HZSM-5 and 0.8 P/Al HZSM-5.

Table S5. NMR deconvolutions with residuals.

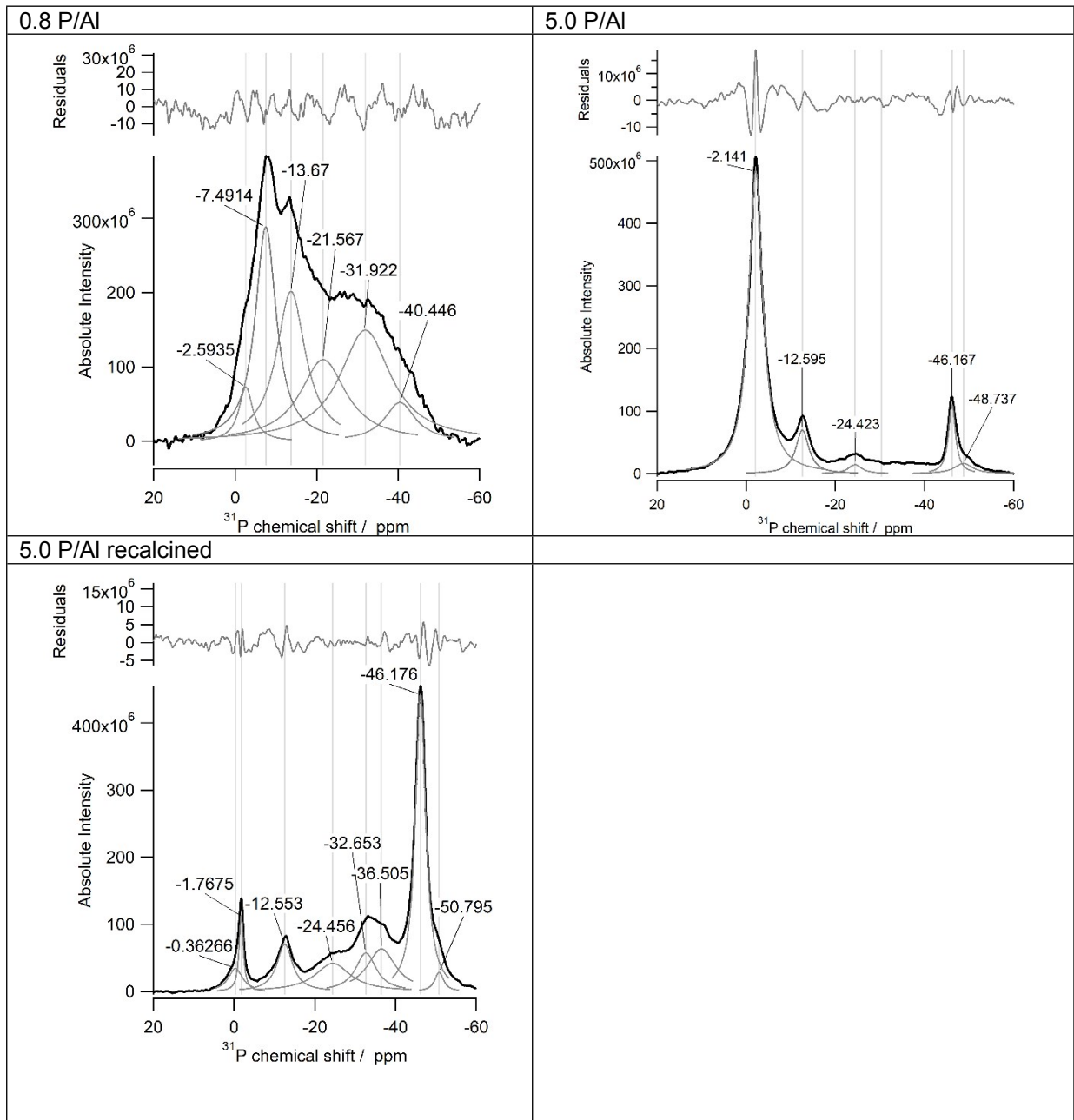
^1H NMR deconvolutions



²⁷Al NMR deconvolutions



³¹P NMR deconvolutions



²⁹Si NMR deconvolutions

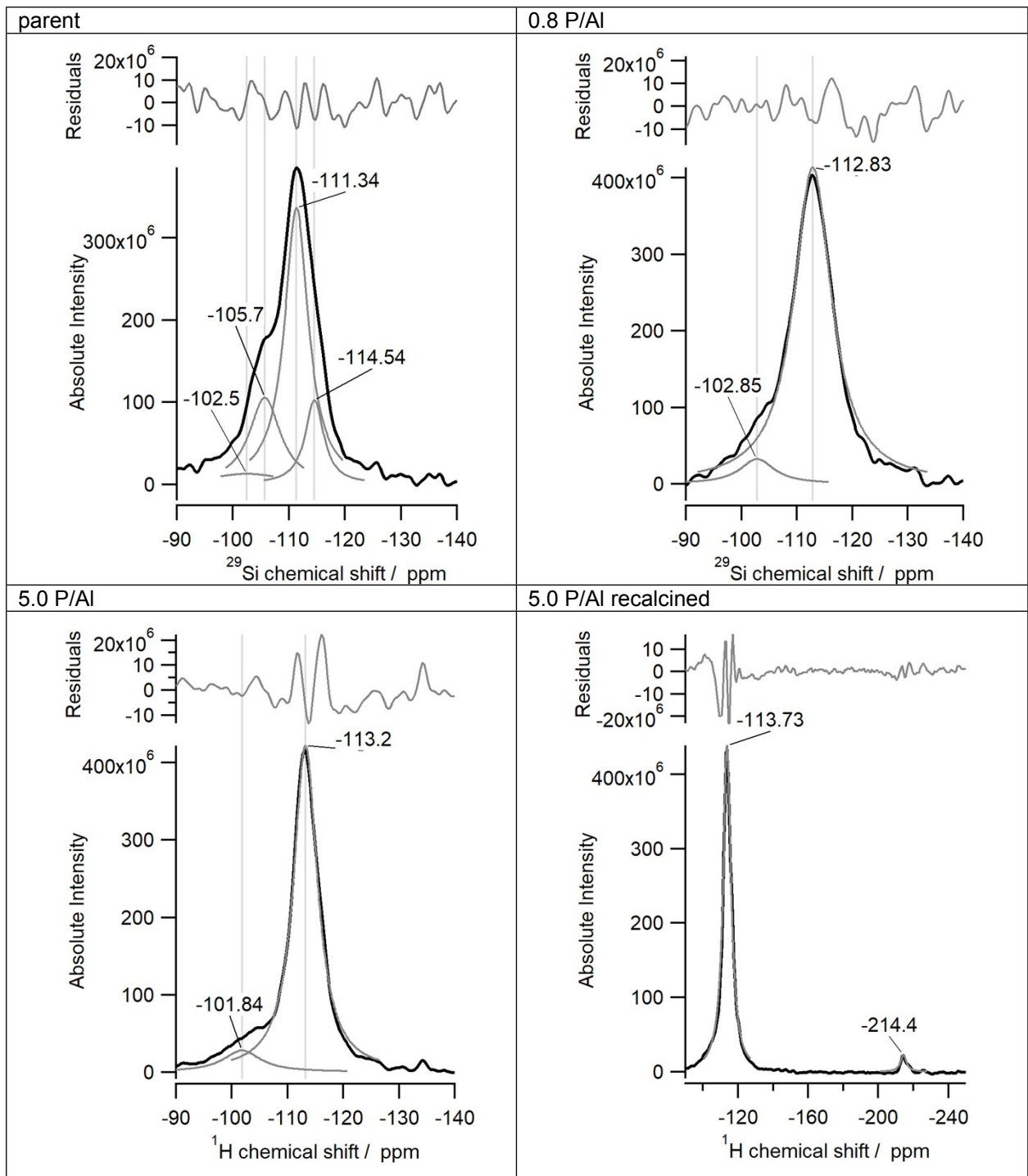


Table S6. Integrated areas of deconvoluted peaks in the ^{27}Al and ^{29}Si NMR spectra.

Spectra	Sample	Resonance	Area
^{27}Al NMR	Parent	54.9	9.69
		-1.5	1.03
	0.8 P/Al	-14.0	28.85
		11.6	11.48
		33.4	16.31
	50.8	5.92	
^{29}Si NMR	Parent	-114.5	1.41
		-111.3	7.30
		-105.7	2.07
		-102.5	0.45
	0.8 P/Al	-112.8	11.64
		-105.7	1.77
	5.0 P/Al	-113.2	7.90
		-101.8	0.20
	5.0 P/Al recalcined	-214.4	0.24
		-113.2	7.80
		-105.7	0.50

References

- 1 A. Le Bail, H. Duroy and J. L. Fourquet, *Mater. Res. Bull.*, 1988, **23**, 447–452.
- 2 R. J. Hill and C. J. Howard, *J. Appl. Crystallogr.*, 1987, **20**, 467–474.
- 3 L. B. Mccusker, R. B. Von Dreele, D. E. Cox, D. Loue È R D and P. Scardi, *Int. Union Crystallogr. J. Appl. Crystallogr. J. Appl. Cryst.*, 1999, **32**, 36–50.
- 4 J. E. Schmidt, J. D. Poplawsky, B. Mazumder, Ā. Attila, D. Fu, D. A. M. de Winter, F. Meirer, S. R. Bare and B. M. Weckhuysen, *Angew. Chemie - Int. Ed.*, 2016, **55**, 11173–11177.
- 5 M. K. Miller and R. G. Forbes, *Mater. Charact.*, 2009, **60**, 461–469.
- 6 L. T. Stephenson, A. V. Ceguerra, T. Li, T. Rojhirunsakool, S. Nag, R. Banerjee, J. M. Cairney and S. P. Ringer, *MethodsX*, 2014, **1**, 12–18.
- 7 M. G. Hetherington and M. K. Miller, *Colloq. Phys.*, 1989, **8**, 535–540.
- 8 D. E. Perea, I. Arslan, J. Liu, Z. Ristanović, L. Kovarik, B. W. Arey, J. A. Lercher, S. R. Bare and B. M. Weckhuysen, *Nat. Commun.*, 2015, **6**, 7589.
- 9 M. P. Moody, L. T. Stephenson, A. V. Ceguerra and S. P. Ringer, *Microsc. Res. Tech.*, 2008, **71**, 542–550.